J Intell Robot Syst (2011) 63:503–523
DOI 10.1007/s10846-010-9524-6

A New Methodology for the Design of Passive Biped Robots: Determining Conditions on the Robot's Parameters for the Existence of Stable Walking Cycles

Paul Vallejos · Javier Ruiz-del-Solar · Francisco Swett

Received: 2 September 2010 / Accepted: 15 December 2010 / Published online: 18 January 2011

Abstract Currently, passive robots are designed following a trial and error process in which the existence of a stable walking cycle for a given passive robot's model is analyzed using Poincaré maps. The standard stability analysis procedure suffers from discretization aliasing, and it is not able to deal with complex passive models. In this paper a methodology that allows finding conditions on the robot's parameters of a given passive model in order to obtain a stable walking cycle is proposed. The proposed methodology overcomes the aliasing problem that arises when Poincaré sections are discretized. Basically, it implements a search process that allows finding stable subspaces in the parameters' space (i.e., regions with parameters' combinations that produce stable walking cycles), by simulating the robot dynamics for different parameters' combinations. After initial conditions are randomly selected, the robot's dynamics is modeled step by step, and in the Poincaré section the existence of a walking cycle is verified. The methodology includes the definition of a search algorithm for exploring the parameters' space, a method for the partition of the space in hypercubes and their efficient management using proper data structures,

P. Vallejos (✉) · J. Ruiz-del-Solar · F. Swett
Department of Electrical Engineering , Universidad de Chile,
Av. Tupper 2007, Santiago, 837-0451, Chile
e-mail: pavallej@ing.uchile.cl

J. Ruiz-del-Solar
e-mail: jruizd@ing.uchile.cl

F. Swett
e-mail: fswett@ing.uchile.cl

P. Vallejos · J. Ruiz-del-Solar
Advanced Mining Technology Center, Universidad de Chile,
Av. Tupper 2007, Santiago, 837-0451, Chile

and the use of so-called design value functions that quantify the feasibility of the resulting parameters. Among the main characteristics of the proposed methodology are being robot independent (it can be used with any passive robot model, regardless of its complexity), and robust (stable subspaces incorporate a stability margin value that deals with differences between the robot's model and its physical realization). The methodology is validated in the design process of a complex semi-passive robot that includes trunk, knees, and non-punctual feet. The robot also considers the use of actuators, controllers and batteries for its actuation.

Keywords Biped robot · Legged locomotion · Passive dynamic walking · Robot dynamics · Stability · Parameters' conditions

1 Introduction

The concept of passive dynamic walking was pioneered by McGeer in the early 1990s [14–20]. In his seminal works, McGeer analyzed the cyclic behavior of purely passive mechanical systems that are able to move in an inclined plane. Cyclic behavior results from the balance between energy losses due to impacts and energy increase due to the slope (gravitational potential energy transformed into kinetic energy) [12].

Research on passive biped robots has increased largely since the seminal works of McGeer [1–6, 10, 11, 13, 25, 27, 28, 31]. In addition to the development of more complex passive models that include trunk, feet, and knees, researchers have proposed semi-passive robots, also called underactuated robots, in order to obtain some degree of control on the robots and to avoid the use of inclined planes [3, 10, 26, 28, 32, 33]. In semi-passive robots energy is injected by actuators instead of gravity. It is worth to mention that the use of actuators contributes not only to the versatility of the robots, but also to the stability of the passive cycles [5, 25]. In addition, inspired on the ideas of passive dynamic walking, there are active robots that use their intrinsic dynamics as a reference for their control. This allows the use of small and simple actuators [35–38]. Resulting robots are able to carry out complex movements, such as playing soccer [39].

Some of the main characteristics of passive and semi-passive robots are energy efficiency, mechanical simplicity, and natural appearance of the resulting gaits [33]. These characteristics are the result of the fact that in passive dynamic walking the robot's control uses the natural dynamics of the robot, instead of trying to restrain it continuously.

Non-trivial passive robot models include feet, knees and trunk, among others parts. Additionally, in order to increase the possibility that a real robot behaves similar to its model, it is necessary to increase the model complexity, including more physical characteristics of the robot. This leads quickly to the impossibility of determining conditions on the robot's parameters[1] required for the existence of a stable

[1]The parameters that define the physical characteristics of the robot, such as masses, lengths and moments of inertia of the different robot's components.

walking cycle. Although some physical characteristics have being associated to the passive walking cycle existence [31], to the best of our knowledge there is not methodology to find the parameters' conditions for a general passive model. Usually, passive robot designers follow a trial and error design process, which typically uses qualitative knowledge about passive walking models (taken from the literature), and in which the existence of a stable walking cycle for the passive robot's model is verified using stability analysis. Stability analysis is normally carried out using Poincaré maps, with the foot impact used as the Poincaré section [7–9, 21–24, 29, 30]. Under this paradigm, stability analysis is carried out by discretizing the Poincaré section using a regular grid. The criterion for the existence of a walking cycle is to look for points in the Poincaré section that are mapped onto themselves, or that after some iterations are finally mapped onto themselves. The methodology has a huge problem: it tends to have aliasing, being very sensitive to the discretization step (grid size). Stable and unstable conditions can be mixed in the same grid point, because of the selected discretization. Thus, it could happen that initial conditions that could cause a robot fall after some steps, could map near enough to be considered as belonging to the same grid point, and therefore part of a stable gait.

We propose that stability analysis of the resulting gaits is a key issue that needs to be incorporated in the design process of passive robots. For this reason a methodology that allows finding conditions on the robot's parameters of a given passive model in order to obtain a stable walking cycle is proposed. The proposed methodology overcomes the aliasing problem because it does not discretize the Poincaré sections. Basically, it implements a search algorithm that allows finding stable subspaces in the parameters' space (i.e., regions with parameters' combinations that produce stable walking cycles), by simulating the robot dynamics for different parameters' combinations. After some initial conditions are randomly selected, the robot's dynamics is modeled step by step, and in the Poincaré section the existence of a walking cycle is verified. Poincaré section's points are classified as stable, unstable and unfeasible. The methodology includes the definition of a search algorithm to explore the parameters' space, a method for the partition of the space in hypercubes and their efficient management using proper data structures, and the use of so-called design value functions that quantify the feasibility of the resulting parameters. Among the main characteristics of the proposed methodology are being (1) robot independent, it can be used with any passive robot model, regardless of its complexity, and (2) robust, stable subspaces incorporate a stability margin that deals with differences between the robot's model and its physical realization.

The methodology is validated in the design process of a complex semi-passive robot that includes trunk, knees, and non-punctual feet. The robot also considers the use of actuators, controllers and batteries for its actuation. Given the fact that our final goal is to build an active robot designed under the passive dynamics paradigm, the robot considers the use of compliant actuators with variable stiffness, built using antagonistic motors and tendons. The actuation of the active robot will be described elsewhere.

The paper is organized as follows. In Section 2, the proposed design methodology is described. In Section 3, the methodology is validated in the design process of a semi-passive robot, which is built using the parameters obtained in simulations. Finally, some conclusions of this work are presented in Section 4.

2 Proposed Design Methodology

2.1 Passive Walking Cycle Analysis Using the Discrete Poincaré Map

In order to analyze the existence of a passive walking cycle for a determinate parameters' set, discrete Poincaré maps,[2] using the foot impact as the Poincaré section,[3] have being used. The discretization usually is a regular grid in all the Poincaré section, which produces aliasing.

In this work, we propose a new discretization of the Poincaré map that overcomes these drawbacks. Given a parameters' set for a passive robot, the proposed discretization consists of randomly choose initial conditions, then simulates the dynamic of the robot using the passive model. If the robot falls before the completeness of the step (any not-foot part of the robot touches the floor or the swinging foot reaches the floor with the knee flexed), then this initial condition is classified as an unfeasible walking condition for this parameters' set. On the contrary, if the step is succesfully completed, then the floor impact is modeled, and a new simulation using the result of the foot-floor collision model as the initial conditions is started. The process is repeated until the robot falls or it completes a certain amount of successful steps. If an initial conditions generates at least one stable step, but the robot finally falls, then it is classified as unstable. On the other hand, if the robot never fall, then consider all the samples involved in the process are classified as stable. This process is repeated until some finalization criteria are fulfilled.

2.2 Global Stability of a Parameters' Set

Using the result of the proposed Poincaré map analysis, a global stability measurement for the sample p of the parameters' subspace s is defined as:

$$global\_stability_p^s = \frac{n_{stable}{}_p^s}{n_{points}{}_p^s} \times \prod_{i=1}^{n_{state}} (\max_i - \min_i)\,. \tag{1}$$

Where $n_{stable}{}_p^s$ is the number of Poincaré map points evaluated in the sample p of the parameters' subspace s that resulted in a stable walking cycle; $\min_i$ and $\max_i$ are the minimal and maximal evaluated value of the i dimension of the initial conditions vector, respectively; $n_{points}{}_p^s$ is the number of Poincaré map points evaluated in the sample p of the parameters' subspace s; and n_{state} is the dimensionality of the state, hence the dimensionality of the initial conditions vector.

Using the previously defined *global_stability*, the stability value of the parameters' subspace s is defined as:

$$subspace\_stability\_value^s = \sum_{p=1}^{n_{eval}{}^s} global\_stability_p^s\,. \tag{2}$$

Where $n_{eval}{}^s$ is the number of samples evaluated in the parameters' subspace s.

[2] A Poincaré map is defined as the intersection of the interest orbits with the Poincaré section. It can be generated using the points of the Poincaré section as the initial conditions of the orbits, and observing the first point in the Poincaré section which the orbits intersects.

[3] A Poincaré section is a lower dimensional subspace of the dynamic system.

2.3 Design Value Function

A robot with a parameters' set that generates a globally stable walking cycle is not necessary easy to construct. Because, for example, it could be hard to have the limbs' center of mass in the foot or in the hip, or it could have some leg's length that give no space for the needed mechanisms.

Due to this, we define a design value function, which represents the feasibility to build a robot with each parameter. In order to give the same importance to every parameter, we use design value functions whose integral over their entire domain is one. For the sake of illustrate this concept, Fig. 1 shows two examples of design value functions used in the design of our semi-passive robot (see Section 3.2): the first one is a pulse design value function used for the Tmp parameter, and the second one is a triangle design value function used for the $CMavgHeight$ parameter.

Once the design value function is defined for each parameter, then the design value of a parameters' space is defined as:

$$design\_value = \prod_{i=1}^{n_{param}} \int_{space_i} design\_value\_function_i \,. \tag{3}$$

Where n_{param} is the number of parameters of the model.

2.4 Parameters' Space Partition

By defining the parameters' space as a $n_{param} - dimensional$ hypercube, we can partition the parameters' space into many subspaces dividing the space by one dimension at time. This partition allows the use of the very computational efficient kd-tree structures for the parameters' space partition representation.

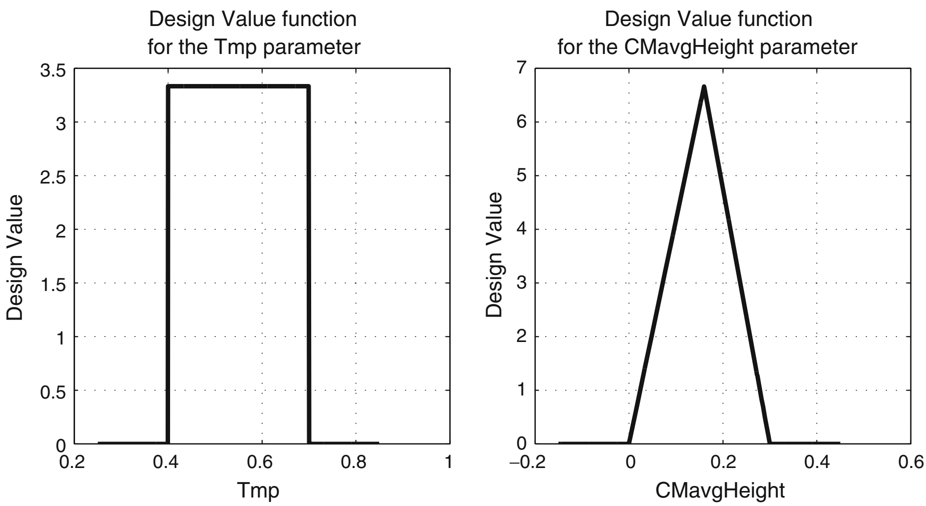

Fig. 1 Examples of design value functions: the *first* is a pulse design value function used for the Tmp parameter, and the *second* is a triangle design value function used for the $CMavgHeight$ parameter

The here proposed methodology looks for the parameters' subspaces with a high design value that contains only parameters with their global stability over a given threshold. Once one of these parameters' subspaces is chosen, the result is not only a stable parameters' set, but a complete range of values for each parameter. This allows to define a stability margin for the design and construction of a real robot, because the real parameters do not need to have exact values, they just need to lay on the range defined by the resulting parameters' subspace. The stability margin is defined as the design value of a parameter's subspace, and it can be considered as an index that can be used to choose which parameter's subspace to use.

2.5 Parameters' Subspace Search Algorithm

In order to find the parameters' subspaces containing only parameters' sets that exhibit a passive walking cycle, we propose the following algorithm:

Generation of an Initial Candidate Subspace The boundaries of the initial candidate subspace are defined as the smallest region of the parameters' space[4] that contain only parameters' sets with a non-zero design value function. The candidate subspace is then populated using parameters' sets obtained by perturbing with gaussian noise stable parameters's sets obtained from a simpler model. For instance, the "Simplest Model" [4] can be used with this purpose. Do this until some minimal amount of stable evaluations have being found.

Searching Phase While at least one candidate subspace with a design value over a given threshold exists do:

1. Select a candidate subspace randomly, using as selection criterion the product between the design value of the subspace and the maximal value between the subspace stability value and a predefined minimal stability value.
2. Randomly choose a parameters' set inside the selected candidate subspace, and calculate its global stability value. If this value is over a given threshold, then the parameters' set is declared as stable, continue to step 3 of "Searching phase". Otherwise, the subspace is divided in two subspaces. The space division is performed on the parameter (belonging to the unstable parameters' set) that generates the parameters' subspace with the largest design value. Go to step 1 of "Searching phase".
3. If the selected candidate subspace has a stability value over a given threshold, then it is declared as a stable subspace, i.e. a subspace with a high design value that contains only parameters with its global stability over a given threshold. The subspace is stored in a list of stable parameters' subspaces.

The stable parameters' subspaces list contains only the parameters' subspaces declared as fully stable. In fact, the kd-tree could still have some parameters' subspaces

[4]The dimensionality of the parameters' space is eleven in the case of the robot to be analyzed (see Section 3.2).

with some stable evaluations (not enough to declare the subspace as fully stable), but these parameters' subspaces have a low design value (the condition to finish is that the kd-tree have no parameters' subspace with a design value over a given threshold). Therefore, these candidate-to-stable parameters' subspaces are not of interest, and it is not relevant whether they are in the stable parameters' subspaces list or not.

It is important to note that as a result of the application of this algorithm all the parameters' sets with a global stability of zero have no passive walking cycle, and they are located in some frontier of two parameters' subspaces. Also, all the parameters' sets with a large design value have a large possibility to be chosen, as a consequence, they have a large possibility to be divided (in the case of unstable subspaces) or to be classified as stable (in the case of stable subspaces).

3 Design Process of a Semi-passive Biped

3.1 Passive Walking Model

Nevertheless the proposed methodology can be applied to any robot model, we validated it with a specific passive biped robot model.

Assuming that the lateral stabilization can be done using an independent controller, we use a bi-dimensional passive model in the sagittal plane. The real robot will have motors, controllers and batteries. All these components will be distributed between the limbs and the trunk. Therefore, the model needs to consider a trunk with mass, two identical legs, with thighs and shanks of different lengths, modeled by a mass and a moment of inertia. The feet are punctual and massless.

For versatility, the active robot will need to exert torque with the feet over the ground. As a consequence, light non-punctual feet will be used. Although the feet torque can be used to stabilize the passive walking cycle [34], they are not needed for its existence and there is always the chance of leaving the supporting ankle unpowered (we will use variable stiffness actuators). Despite the fact that the model considers punctual massless feet, the mass of the feet will be considered as part of the shanks.

We model the walking cycle as a sequence of four stages: (1) flexed knee swinging stage, (2) instantaneous knee impact, (3) blocked knee swinging stage, and (4) instantaneous foot impact.

Following McGeer's work [16], we define the pseudo frequency ω as:

$$\omega = \sqrt{\frac{g}{Leg\,Length}}\,. \tag{4}$$

The use of the pseudo frequency ω and the normalized values of masses and lengths eliminates the total mass and the leg length from the dynamic equations, making them dependent only on ω [16]. Therefore, the normalized parameters are:

$$thigh\,Length\,Percentage = \frac{thigh\,Length}{Leg\,Length}\,. \tag{5}$$

$$shank\,Length\,Percentage = \frac{shank\,Length}{Leg\,Length}\,. \tag{6}$$

$$thighLengthCMxPercentage = \frac{thighLengthCMx}{LegLength}. \tag{7}$$

$$thighLengthCMyPercentage = \frac{thighLengthCMy}{LegLength}. \tag{8}$$

$$shankLengthCMxPercentage = \frac{shankLengthCMx}{LegLength}. \tag{9}$$

$$shankLengthCMyPercentage = \frac{shankLengthCMy}{LegLength}. \tag{10}$$

$$trunkMassPercentage = \frac{mTrunk}{TotalMass}. \tag{11}$$

$$thighMassPercentage = \frac{mThigh}{TotalMass}. \tag{12}$$

$$shankMassPercentage = \frac{mShank}{TotalMass}. \tag{13}$$

$$thighInertiaPercentage = \frac{Ithigh}{LegLength^2 \cdot TotalMass}. \tag{14}$$

$$shankInertiaPercentage = \frac{Ishank}{LegLength^2 \cdot TotalMass}. \tag{15}$$

Where, $thighLength$ and $shankLength$ are the lengths of the thigh and the shank; $thighLengthCMx$ and $thighLengthCMy$ are the x and y coordinates of the thigh mass center referenced from the hip; $shankLengthCMx$ and $shankLengthCMy$ are the x and y coordinates of the shank mass center referenced from the knee; $mTrunk$, $mThigh$, and $mShank$ are the masses of the trunk, thigh, and shank respectively. $LegLength$ and $TotalMass$ are, respectively, the total length of the leg and the total mass of the robot. They are formally defined as:

$$LegLength = thighLength + shankLength. \tag{16}$$

$$TotalMass = mTrunk + 2 \cdot (mThigh + mShank). \tag{17}$$

We define our global coordinate system located on the stand foot with the y axis normal to the floor, and the x axis parallel to the floor surface. In this system, we define $\overrightarrow{CMx}(t)$ as the vector with the x coordinates of all the centers of mass; $\overrightarrow{CMh}(t)$ as the vector with the y coordinates of all the centers of mass; and $\overrightarrow{masses}$ as the vector with all the masses. Then, the potential energy $V(t)$ is defined as:

$$V(t) = g \cdot \overrightarrow{masses}^T \cdot \left(\overrightarrow{CMh}(t) \cdot \mathrm{Cos}(\alpha) - \overrightarrow{CMx}(t) \cdot \mathrm{Sin}(\alpha)\right). \tag{18}$$

Defining a virtual gravity as:

$$g^v = g \cdot \mathrm{Cos}(\alpha). \tag{19}$$

Then, the potential energy can be expressed as:

$$V(t) = g^v \cdot \overrightarrow{masses}^T \cdot \overrightarrow{CMh}(t) - g^v \cdot \mathrm{Tan}(\alpha) \cdot \overrightarrow{masses}^T \cdot \overrightarrow{CMx}(t). \tag{20}$$

Equation 20 can be interpreted as if the potential energy was compounded by one virtual vertical potential energy and one virtual horizontal potential energy in the coordinate system aligned with the slope.

Defining $\overrightarrow{inertia}$ as the vector with all the moments of inertia, and $\overrightarrow{q}(t)$ as the vector with all the orientations of the segments (trunk, thighs and shanks), defined with respect to the floor plane. Then, the kinetic energy of the robot is expressed as:

$$K(t) = \frac{\overrightarrow{masses}^T \cdot \left(\left(\frac{\partial \overrightarrow{CMh}(t)}{\partial t}\right)^2 + \left(\frac{\partial \overrightarrow{CMx}(t)}{\partial t}\right)^2 \right)}{2} + \frac{\overrightarrow{inertia}^T \cdot \left(\frac{\partial \overrightarrow{q}(t)}{\partial t}\right)^2}{2}. \tag{21}$$

We define the state vector of the model with three dimensions: (1) the angle θ between the shank and the floor normal, (2) the angle ϕ between the two thighs, and (3) the knee angle γ of the swinging leg. Then, the dynamic equations can be obtained using the Lagrange method. In our case, the Lagrange equations are:

$$\frac{d}{dt}\left(\frac{\partial\left(K(t) - V(t)\right)}{\theta'(t)}\right) - \frac{\partial\left(K(t) - V(t)\right)}{\partial\theta(t)} = 0. \tag{22}$$

$$\frac{d}{dt}\left(\frac{\partial\left(K(t) - V(t)\right)}{\phi'(t)}\right) - \frac{\partial\left(K(t) - V(t)\right)}{\partial\phi(t)} = 0. \tag{23}$$

$$\frac{d}{dt}\left(\frac{\partial\left(K(t) - V(t)\right)}{\gamma'(t)}\right) - \frac{\partial\left(K(t) - V(t)\right)}{\partial\gamma(t)} = 0. \tag{24}$$

The flexed knee swinging stage is ruled by Eqs. 22, 23, and 24. On the other hand, the blocked knee swinging stage is ruled by Eqs. 22, 23, $\gamma = 0$, and $\gamma' = 0$ (the knee is blocked).

Both the knee impact and the foot impact are modeled as perfectly inelastic collisions. There is no energy conservation, but there is moment conservation. The moment conservation in kneed walking robots has being very well explained in the literature [11]. We used the same model utilized by Hsu-Chen in her thesis [11], but also considering the moment of inertia.

Using the dynamic equations of the flexed knee swinging stage and the blocked knee swinging stage, as well as the model of the knee impact and the foot impact, a full walking cycle can be simulated and analyzed.

3.2 Parameters' Space Reduction

In order to reduce the parameters' space complexity as much as possible, and to obtain a scale-invariant model (only torques depends on robot mass and height), eleven simplified parameters can be defined that fully specify the previously described model. The reduced parameters are:

$$Slope = \mathrm{Tan}(\alpha). \tag{25}$$

$$Tmp = trunkMassPercentage. \tag{26}$$

$$Lmr = \mathrm{ArcTan}\left(\frac{thighMassPercentage}{shankMassPercentage}\right). \tag{27}$$

$$CMavgHeight = \frac{thighLengthCMy + shankLengthCMy}{2}. \tag{28}$$

$$CMheightDif = thighLengthCMy - shankLengthCMy\,. \tag{29}$$

$$Tlp = thighLengthPercentage\,. \tag{30}$$

$$ShankCMx = shankLengthCMx\,. \tag{31}$$

$$ThighCMx = thighLengthCMx\,. \tag{32}$$

$$ShankInertia = shankInertiaPercentage\,. \tag{33}$$

$$ThighInertia = thighInertiaPercentage\,. \tag{34}$$

$$\omega = \sqrt{\frac{g}{LegLength}}\,. \tag{35}$$

Since it is not intuitive to understand the *Lmr* parameter's function, Fig. 2 shows the function from the *Lmr* parameter to the relation between the thigh mass and the shank mass.

3.3 Stable Parameters' Subspaces Analysis

Given the fact that the parameters' subspace search algorithm finds the stable parameters' subspaces after using a sampling process (see Section 2.5), it is important to evaluate several parameters' sets in order to obtain the stable parameters' subspaces using the proposed methodology with our passive walking model (see Section 3.1). We evaluated 3,407,519 parameters' sets during the application of the proposed methodology. 2,605,233 of them where classified as stable parameters' sets and 802,286 as unstable parameters' sets. A total of 2,940 parameters' subspaces were found having only stable parameters' sets and a design value large enough. As it was stated in Section 2.5, stable parameters' sets are more likely to be evaluated since the algorithm gives a higher selection probability to more stable parameters' subspaces and to those that have a larger design value. For the purpose of analyzing the goodness of the proposed methodology, the process of finding the parameters' subspaces will be called training, resembling a statistical classifier. The result of the proposed methodology can be interpreted as a classifier of parameters' sets in two

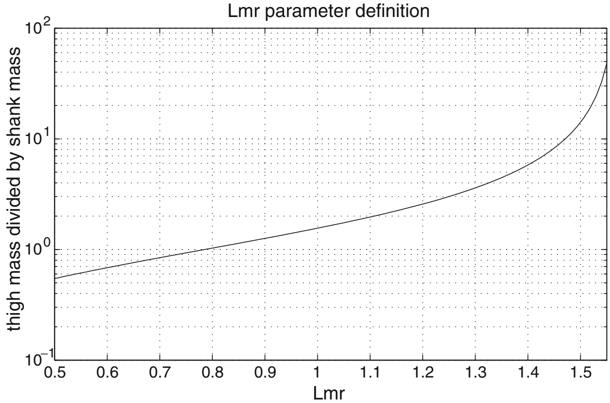

Fig. 2 Function from the *Lmr* parameter to the relation between the thigh mass and the shank mass

classes: (1) stable (with a passive walking cycle), and (2) unstable (without a passive walking cycle).

It is important to notice that, since the essentials of the passive walking dynamics can be observed in the “simplest model” [31], then the generalization of its results to our model have a large probability of being stable under our model. Therefore, in the generation of an initial candidate subspace of the parameters’ subspace search algorithm (see Section 2.5), the algebraic solutions of the “simplest model”, perturbed using gaussian noise, are used as initial conditions in the first simulations, in order to accelerate the system convergence.

In order to validate the proposed methodology, we evaluated 30,000 new parameters’ sets. To accomplish this, 300 subspaces were randomly selected, each one of them with 100 parameters’ sets evaluations. We evaluated each parameters’ set observing its stability. This process is called the validation stage (in the same sense of an statistical classifier).

We analyzed the performance of the proposed system by observing the relationship between the number of stable evaluations of the parameters’ sets subspaces in the training stage, and the percentage of stable evaluations in the validation stage. Figure 3 shows this relationship. As expected, we see a high correlation between the stability in training and validation. This means that there is a high probability that a parameters’ set contained in one of the stable parameters’ subspaces found using the proposed methodology is stable. This validation is important, because as mentioned, the parameters’ subspaces are generated using a sampling process.

3.4 Using the Methodology Results in the Design of a Real Semi-passive Biped Robot

As a first stage for the design of a real robot based on our biped passive walking model, we selected some stable parameters’ subspaces, using their stability margin (defined as equals to the design value) as the selection probability. Then, we analyzed the parameters’ conditions of these subspaces and we deduced the following keys conditions for the rough design of the robot: (1) More than half of the mass must be in the trunk, (2) The mass of the thigh must be between 3 and 4 times the shank

Fig. 3 Validation results for the parameters’ subspaces classification

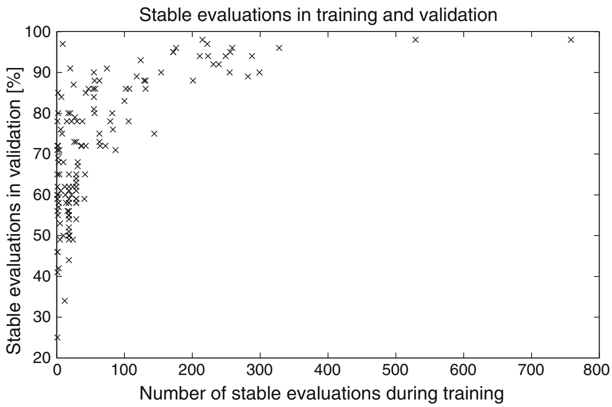

mass, and (3) The shank and thigh must have their centers of mass around the middle of the segment. Only three parameters were used to draw these rough conclusions: Tmp, Lmr, and $CMavgHeight$. The conditions for these three parameters in fifteen selected subspaces are shown in Table 1. It is important to mention that these results are concordant with results already obtained in the literature with other passive walking models [11].

In a second stage, the design of the active robot that should exhibit a passive walking cycle and fulfill the coarse parameters' conditions is carried out. Due to the masses conditions, we decided to put the hip motors in the trunk, and the knee and ankle motors in the thigh. The selected actuators are two antagonistic brushless DC motors for each degree of freedom, each of which drives a twisting rope to pull a tendon. This actuator selection is a low mass solution that allows the location of the motors wherever helps the accomplishment of the parameters' conditions. Also this kind of actuation is stiffness variable, so the control system can decide to leave any joint free at any time.

Once a first version of the design was ready, we analyzed its actual physical parameters in order to verify whether they belong to one of our stable subspaces. Given the fact that the process of making a semi-passive robot involves several aspects, like the motor placement, the election of the used materials, the shape of the parts, the location of the joints, among others, making the robot to accomplish with the parameters' conditions is very hard. Consequently, the parameters of the first version of the design do not belong to any stable subspace. But, due to the stability margin, looking for stable subspaces near our actual robot parameters' set is straightforward. In this way, we look for a stable subspace near our actual robot parameters' set by

Table 1 Conditions for the three parameters used to deduce the keys for the rough design in 15 selected subspaces (see Fig. 2 for the interpretation of the Lmr parameter)

	Tmp		Lmr		$CMavgHeight$		Stability	Stable	Design
	Min	Max	Min	Max	Min	Max		evaluations	value
	0.47	0.70	1.25	1.28	0.25	0.46	0.33	18	1,151.40
	0.44	0.50	1.08	1.10	0.17	0.40	0.39	29	688.48
	0.57	0.71	1.25	1.27	0.22	0.47	2.01	222	59.09
	0.56	0.60	1.27	1.38	0.26	0.42	2.03	65	29.74
	0.62	0.62	1.32	1.35	0.26	0.26	2.24	131	0.24
	0.37	0.55	1.28	1.31	0.22	0.43	2.27	155	0.19
	0.41	0.46	1.25	1.30	0.19	0.30	2.19	243	0.17
	0.56	0.59	1.33	1.37	0.27	0.27	1.92	114	0.16
	0.57	0.59	1.22	1.25	0.23	0.48	1.30	249	0.15
	0.61	0.69	1.15	1.25	0.28	0.41	0.27	56	0.15
	0.57	0.66	1.33	1.33	0.17	0.26	2.20	277	0.13
	0.54	0.54	1.27	1.37	0.29	0.42	1.01	79	0.12
	0.43	0.64	1.26	1.29	0.21	0.29	0.39	33	0.11
	0.48	0.63	1.08	1.08	0.24	0.41	1.11	56	0.09
	0.55	0.65	1.27	1.34	0.27	0.30	0.34	30	0.09
Avg.	0.52	0.61	1.24	1.29	0.24	0.37	1.33	117	128.69
Min.	0.37	0.46	1.08	1.08	0.17	0.26	0.27	18	0.09
Max.	0.62	0.71	1.33	1.38	0.29	0.48	2.27	277	1,151.40

observing all the stable subspaces in which our robot accomplish all but one or two rules. This gives more than 1,000 possible stable subspaces. From them we selected only those with a subspace stability value over a certain threshold, obtaining around 20 alternatives. Finally, we selected the easiest condition to accomplish with minor changes, this was adding mass to the thigh near the knee. Then, our actual mechanical robot design accomplished all the parameters' conditions of a stable subspace found using our design methodology. Next, we analyze its passive walking cycle behavior.

The Poincaré map generated with our model for the corrected robot parameters is very useful for the passive walking cycle analysis. The evaluations of the Poincaré map can be grouped according to their stability into stable walking cycles, unstable walking cycles, and unfeasible walking. Figure 4 shows the grouped Poincaré map, where the stable walking cycles area is easily recognized. It is important to notice that due to the selection of the foot impact as the Poincaré section, the Poincaré section is determined only by some components of the state. The foot impact take place with the knee blocked. Therefore, both the angle of the knee γ and its derivative γ' are equal to zero. Also, during the foot impact, both feet are on the floor, hence the angle between the legs ϕ is twice the angle of the standing leg θ. As a consequence, in our model the Poincaré section is fully defined by the angular position θ, and the angular speeds θ' and ϕ'. The dependence of the Poincaré section on ϕ' is given by the effect of the moment of inertia of the swinging leg with respect to the impact point. Thus, assuming that the moment of inertia of the swinging leg is negligible with respect to the sum of the moments of inertia of the trunk and the standing leg, the results of the "simplest model" [4] can be applied:

$$\phi' = 2 \cdot \mathrm{Sin}(\theta)^2 \cdot \theta' . \tag{36}$$

Given that the Poincaré section can be any subspace of the dynamic system with a lower dimensionality, we define the Poincaré section as a two dimensional space accomplishing all the restrictions for the foot impact shown in the previous paragraph, including the restriction of Eq. 36. Consequently, the Poincaré section is defined by θ and θ'.

Stable, unstable, and unfeasible walking cycles areas can be distinguished in the grouped Poincaré map. Nevertheless, in order to see the differences inside a region, a

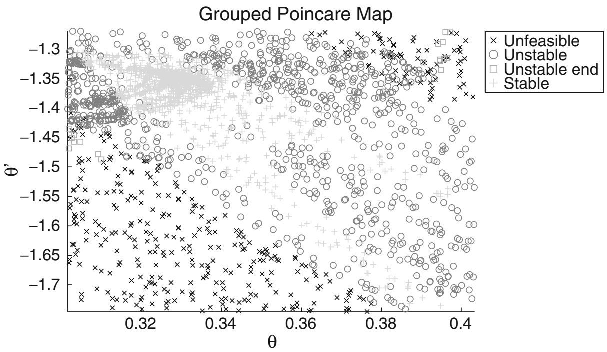

Fig. 4 Poincaré map with the evaluations grouped in stable walking cycles, unstable walking cycles and unfeasible walking

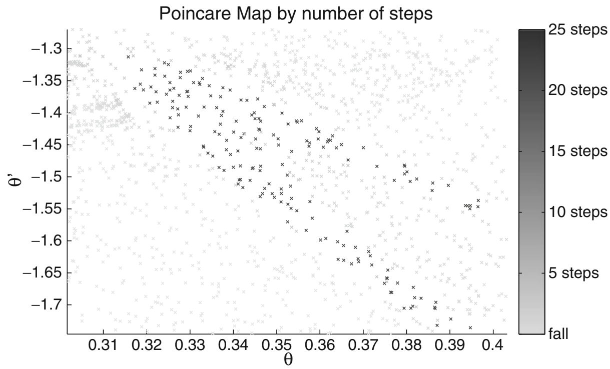

Fig. 5 Poincaré map. The number of steps of each evaluation is shown in *gray scale*

Poincaré map with the number of successful steps of each evaluation as the intensity of each point is shown in Fig. 5, where the stability distribution in the Poincaré map can be appreciated.

Also, a similar approach can be used to analyze the stable walking cycle area. Since we stop simulating after a determined number of successful steps, each stable walking cycle has a fixed length. Figure 6 presents a Poincaré map with only the stable walking cycles area using the position of each point in its cycle as its intensity. This plot illustrates the existence of one accumulation point and its shape.

Once the stable accumulation points have being identified, we can select the appropriated initial conditions for our robot. Finally, we simulate these initial conditions to verify the passive walking cycle and to analyze in detail the walking cycle behavior. Figure 7 shows the initial conditions of all the given steps in the Poincaré map together with its trajectory. It can be seen that the walking started near the stable cycle, and quickly converged to the accumulation point, performing a stable passive walk. Figure 8 shows the first 6 steps of the obtained walking cycle. A very natural walk is seen.

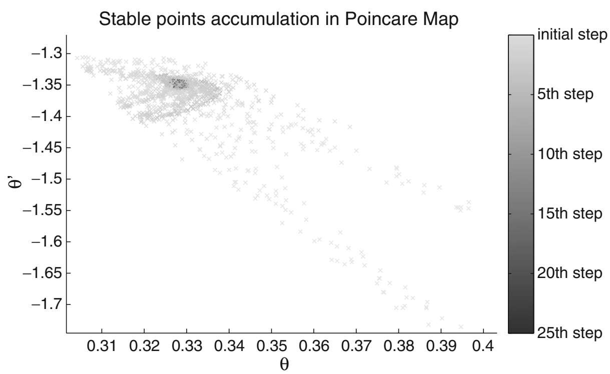

Fig. 6 Points of the Poincaré map that belong to some stable evaluation. The *gray scale* shows the position of the point in the evaluation

Fig. 7 Simulation of the selected walking cycle in the Poincaré map. On the *bottom*, the points belonging to some stable evaluation are shown. The *gray scale* represents the position of the point in the evaluation

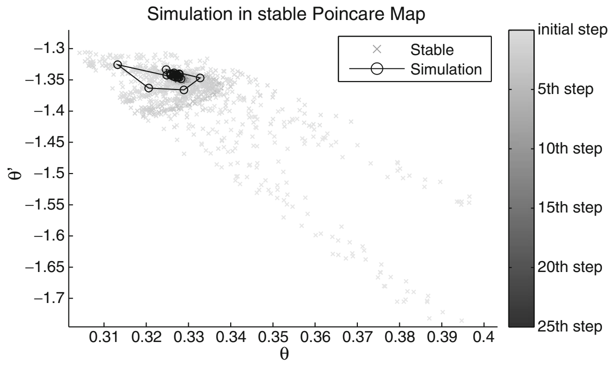

An inspection of the phase space (Fig. 9) of the simulated robot gives an insight into the behavior of the walking cycle. The knee and foot impact can be appreciated as discontinuities in the speeds. We can interpret the system as a system compounded by the kinetic energy and the virtual vertical potential energy loosing kinetic energy in each impact, but earning energy from the virtual horizontal potential energy. When the system is inside a passive walking cycle, the kinetic energy lost in each impact must be equal to the energy acquired from the virtual horizontal potential energy. Figure 10 shows the virtual vertical potential energy and kinetic energy plot. All phase space plots and the energy plot are followed by the passive walking model clockwise. Discontinuities in angular speeds or kinetic energy on these plots mean foot impacts or knee impacts. In the energy plot (Fig. 10), the largest discontinuity is the foot impact, that generates a big kinetic energy lost. It is followed by the free knee swinging stage, in which the energy is increasing due to the non plotted virtual horizontal potential energy. Next, there is a smaller discontinuity that shows the knee impact that generates a smaller kinetic energy lost. Finally, there is the blocked knee swinging stage, also with an increase of the total energy due to the non plotted virtual horizontal potential energy. This plot shows clearly an orbit that in short term varies the total energy, but in long term it keeps it constant, because the kinetic energy lost in impacts is compensated by the potential energy injected to the system by the virtual horizontal potential energy.

Another important characteristic of a walking cycle is its displacement speed. It can be seen in Fig. 11. The displacement speed is important for the robotic

Fig. 8 Six first steps of the simulation

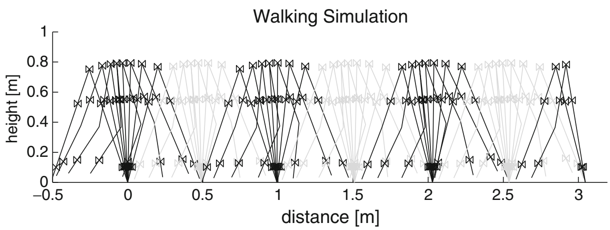

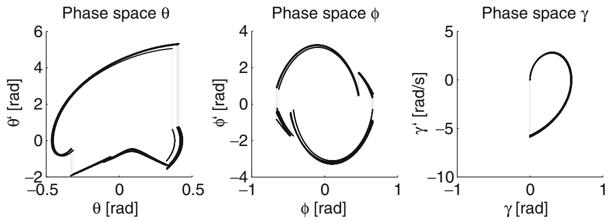

Fig. 9 Phase space of the robot during the simulation

applications and should be dependent on the slope [16]. We will compare this feature with the results on the mechanical design simulation.

3.5 Final Mechanical Design of the Real Semi-passive Biped Robot

The mechanical design of the real robot, with the parameters' subspace obtained using the here proposed methodology is done using Solidworks®. The real physical robot is mechanically built (see Fig. 12b), and we are currently working in the design of the controllers of the actuators in charge of the lateral stabilization, and of providing the energy of the slope when the robot is walking on even floor. Therefore, we still do not have a real-world validation of our methodology, and our passive model. Nevertheless, we used the simulation engine available in the Solidworks® software as an external validation for both the proposed methodology, and the used model. Figure 12 shows the mechanical design of the actual robot with the parameters' set obtained using the here proposed methodology, and the real robot built using the mechanical design. By observing Fig. 12, it can be noted that the mechanical design has anthropomorphic feet while the model used in the proposed methodology validation has punctual feet. The mechanical model feet are lightweight, making the torque needed to keep the swinging foot parallel to the floor negligible. Also, the standing foot actuator will be turned off or it will be used to increase the stability of the passive walking cycle. In conclusion, neither the swinging foot nor the standing foot will affect the existence or the performance of the passive

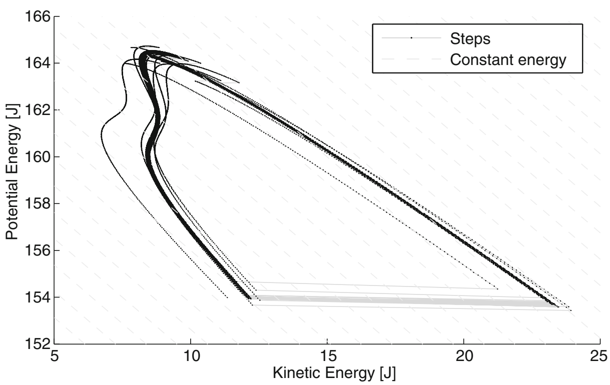

Fig. 10 Virtual vertical potential energy and kinetic energy of the robot during the simulation

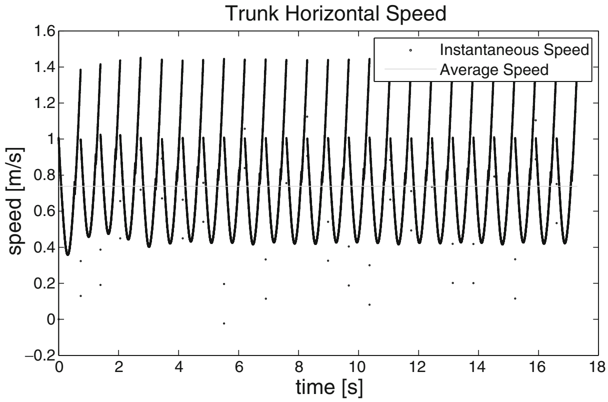

Fig. 11 Horizontal speed of the robot's trunk during the simulation

walking cycle. On the contrary, the feet are needed for the independent lateral stabilization.

Looking at the Poincaré map for the actual robot parameters' set, the initial conditions of the stable walking cycle can be established. The initial simulations performed on the Solidworks® mechanical simulator did not show a stable walking cycle. However, after a small variation of the slope, the mechanical model of the robot exhibits a stable walking cycle. This walking cycle is not equal, but very similar to the simulated previously with our model. It looks very natural and stable. Figure 13 shows the first five steps of the mechanical model simulation walk.

The phase space of the actual robot mechanical design simulated in the mechanical simulator is shown in Fig. 14. Also, the trunk horizontal speed is shown in Fig. 15. These plots reveal that the robot started not to close to the stable orbit, but converged in a few steps to the stable passive walking cycle.

(a) (b)

Fig. 12 **a** Mechanical model of the robot with the parameters' sets obtained using the here proposed methodology. **b** Real robot built using the mechanical design

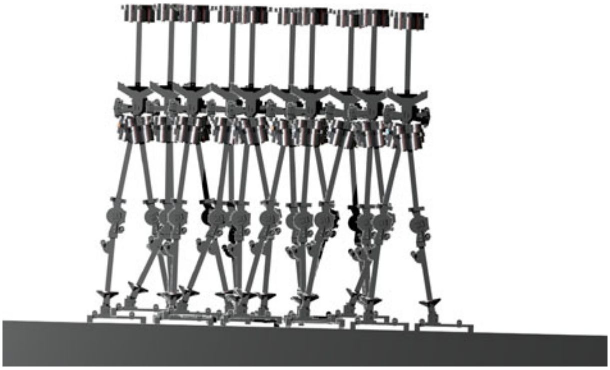

Fig. 13 Five first steps of the mechanical model walk

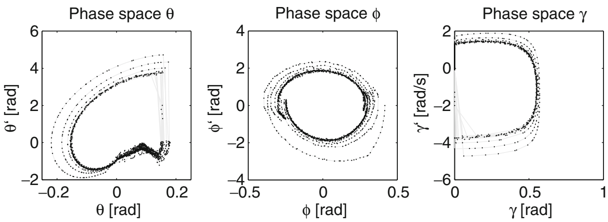

Fig. 14 Phase space of the actual robot mechanical design

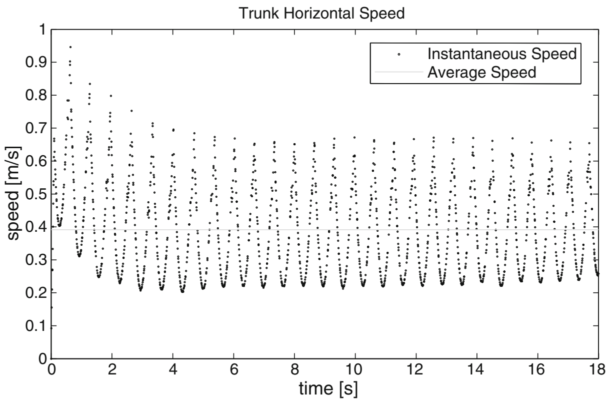

Fig. 15 Horizontal speed of the actual robot mechanical design

The similitudes between the phase space of the model simulation and the phase space of the actual robot mechanical design are evident. There are some minor dissimilarities in its shape and a large difference in the step amplitude. This is explained by the slope difference: the model simulation used a slope of 4.85°, while the actual robot mechanical simulation used a slope of 1.7°. It was not possible to simulate both using the same slope. Probably this was due to the impact losses: instantaneous collisions were used in the model simulations, while elastic collisions with some deformations were used by the Solidworks® mechanical simulator. This make the energy losses very larger in the model simulations, needing a larger slope. It is widely known that a larger slope generates a larger step amplitude in the passive walking cycle [16]. As a consequence, the model simulation exhibits a larger step amplitude than the actual robot mechanical design simulation.

In his work, McGeer predicted that the step time depends only on gravity and leg length [16]. Consequently, despite the large slope difference between the simulations with our model and the simulation on the Solidworks® mechanical simulator, the step time differs only in approximately 5%. This, in conjunction with the difference in step amplitude mentioned in the previous paragraph, explains why the trunk horizontal speed of the model simulation is almost twice the horizontal speed of the mechanical design simulation on the Solidworks® mechanical simulator.

4 Conclusions and Discussions

A new methodology for finding the parameters' conditions that permits the existence of a stable passive walking cycle was proposed in this paper. The methodology can be used with any passive walking model regardless of its complexity. The proposed methodology overcomes the aliasing problem that arises when Poincaré sections are discretized. The result of applying the proposed methodology is a set of rules that the robot's parameters must obey in order to exhibit a passive walking cycle. The resulting set of rules is presented as a parameters' subspace with a stability margin index (also referred as design value), which allows choosing between different resulting parameters' subspaces. The authors have no knowledge of any other methodology that can be used on an arbitrary passive biped model in order to find the parameters' conditions needed for the existence of a passive walking cycle.

The proposed methodology was successful in the design process of a semi-passive biped robot. It allowed finding the parameters' conditions for the existence of a passive walking cycle. These results were exhaustively validated using computational simulations of our passive walking model. Also, the resulting parameters were validated in an external mechanical simulator with a much more complex robot model. The resulting parameters' conditions allowed us to easily design, and successfully built a robot that, at least in the mechanical design simulations, exhibits a passive walking cycle.

Although the simulated model and the mechanical design simulation exhibit the passive walking cycle with slightly different parameters (apparently because the differences due to the model used in our implementation and the model of the mechanical simulation software), a slight increment of the slope corrected the difference, leading to the appearance of the predicted passive walking cycle.

Testing the resulting parameters' conditions in reality is future work. To accomplish this, our research group is currently implementing the lateral stabilization subsystem of the semi-passive biped robot (see Fig. 12).

Acknowledgements This research work was partially funded by the doctoral grant program of CONICYT (Chile), by MECESUP Project FSM 0601, and by FONDECYT project 1090250.

References

1. Coleman, M.J.: A stability study of a three-dimensional passive-dynamic model of human gait. Ph.D. Thesis, Cornell University (1998)
2. Collins, S.H., Wisse, M., Ruina, A.: A three-dimensional passive-dynamic walking robot with two legs and knees. Int. J. Rob. Res. **20**(7), 607–615 (2001)
3. Collins, S., Ruina, A., Tedrake, R., Wisse, M.: Efficient bipedal robots based on passive-dynamic walkers. Science **307**(5712), 1082–1085 (2005)
4. Garcia, M.: Stability, scaling, and chaos in passive-dynamic gait models. Ph.d. Thesis, Sibley School of Mechanical and Aerospace Engineering, Cornell University (1999)
5. Goswami, A., Espiau, B., Keramane, A.: Limit cycles and their stability in a passive bipedal gait. In: Proceedings of the IEEE 1996 International Conference on Robotics and Automation, vol. 1, pp. 246–251. Minneapolis, USA (1996)
6. Goswami, A., Goswami, A., Thuilot, B., Thuilot, B., Espiau, B., Espiau, B.: Compass-like Biped Robot—Part i: Stability and bifurcation of passive gaits. Tech. Rep. 2996, INRIA: Institut National de Recherche en Informatique et en Automatique (1996)
7. Grizzle, J., Plestan, F., Abba, G.: Poincare's method for systems with impulse effects: application to mechanical biped locomotion. In: Proceedings of the 38th IEEE Conference on Decision and Control, vol. 4, pp. 3869–3876 (1999)
8. Grizzle, J., Abba, G., Plestan, F.: Asymptotically stable walking for biped robots: analysis via systems with impulse effects. IEEE Trans. Automat. Contr. **46**(1), 51–64 (2001)
9. Grizzle, J., Abba, G., Plestan, F.: Correction to "asymptotically stable walking for biped robots: analysis via systems with impulse effects". IEEE Trans. Automat. Contr. **46**(3), 513–513 (2001)
10. Haruna, M., Ogino, M., Hosoda, K., Asada, M.: Yet another humanoid walking—passive dynamic walking with torso under simple control. In: Proceedings of the 2001 IEEE International Conference on Intelligent Robots and Systems, vol. 1, pp. 259–264 (2001)
11. Hsu Chen, V.: Passive dynamic walking with knees: a point foot model. Master Thesis, Department of Electrical Engineering and Computer Science, Massachusetts Institute of Technology (2007)
12. Kajita, S., Espiau, B.: Springer Handbook of Robotics, 1st edn., chap. 16, pp. 361–389. Springer (2008)
13. Kuo, A.D.: Stabilization of lateral motion in passive dynamic walking. Int. J. Rob. Res. **18**(9), 917–930 (1999)
14. McGeer, T.: Passive dynamic walking. Tech. Rep. CSS-ISS TR 88-02, Simon Fraser University, Burnaby, British Columbia, Canada (1988)
15. McGeer, T.: Passive bipedal running. In: Proceedings of the Royal Society of London, Series B, Biological Sciences, vol. 240, pp. 107–134 (1990)
16. McGeer, T.: Passive dynamic walking. Int. J. Rob. Res. **9**(2), 62–82 (1990)
17. McGeer, T.: Passive walking with knees. In: Proceedings of the 1990 IEEE International Conference on Robotics and Automation, vol. 3, pp. 1640–1645 (1990)
18. McGeer, T.: Principles of Walking and Running. Advances in Comparative and Environmental Physiology, vol. 11, chap. 4. Springer-Verlag (1992)
19. McGeer, T.: Dynamics and control of bipedal locomotion. J. Theor. Biol. **163**, 277–314 (1993)
20. McGeer, T.: Passive dynamic biped catalogue, 1991. In: Proceedings of the 2nd International Symposium on Experimental Robotics II, pp. 465–490. Springer-Verlag, London, UK (1993)
21. Morimoto, J., Atkeson, C.: Learning biped locomotion. IEEE Robot. Autom. Mag. **14**(2), 41–51 (2007)
22. Morris, B., Grizzle, J.: A restricted Poincaré map for determining exponentially stable periodic orbits in systems with impulse effects: application to bipedal robots. In: 44th IEEE Conference

on Decision and Control and 2005 European Control Conference. CDC-ECC '05, pp. 4199–4206 (2005)

23. Morris, B., Grizzle, J.: Hybrid invariance in bipedal robots with series compliant actuators. In: 45th IEEE Conference on Decision and Control, pp. 4793–4800 (2006)
24. Morris, B., Grizzle, J.: Hybrid invariant manifolds in systems with impulse effects with application to periodic locomotion in bipedal robots. IEEE Trans. Automat. Contr. **54**(8), 1751–1764 (2009)
25. Ohta, H., Yamakita, M., Furuta, K.: From passive to active dynamic walking. In: Proceedings of the 38th IEEE Conference on Decision and Control, vol. 4, pp. 3883–3885 (1999)
26. Paul, C., Yokoi, H., Matsushita, K.: Design and control of humanoid robot locomotion with passive legs and upper body actuation. In: Proceedings of the International Symposium on Robotics. Paris, France (2003)
27. Pratt, J.: Exploiting inherent robustness and natural dynamics in the control of bipedal walking robots. Ph.d. Thesis, Department of Electrical Engineering and Computer Science, Massachusetts Institute of Technology (2000)
28. Tedrake, R.: Actuating a simple 3d passive dynamic walker. In: Proceedings of the IEEE International Conference on Robotics and Automation, pp. 4656–4661 (2004)
29. Westervelt, E., Grizzle, J., Koditschek, D.: Hybrid zero dynamics of planar biped walkers. IEEE Trans. Automat. Contr. **48**(1), 42–56 (2003)
30. Westervelt, E.R., Grizzle, J.W., Chevallereau, C., Choi, J.H., Morris, B.: Feedback Control of Dynamic Bipedal Robot Locomotion. CRC Press, Boca Raton, FL (2007)
31. Wisse, M.: Essentials of dynamic walking—analysis and design of two-legged robots. Ph.d. Thesis, Faculty of Mechanical Engineering, Technische Universiteit Delft (2004)
32. Wisse, M.: Three additions to passive dynamic walking; actuation, an upper body, and 3d stability. In: Proceedings of the 2004 IEEE International Conference on Humanoid Robots, vol. 1, pp. 113–132 (2004)
33. Wisse, M., Feliksdal, G., Van Frankkenhuyzen, J., Moyer, B.: Passive-based walking robot. IEEE Robot. Autom. Mag. **14**(2), 52–62 (2007)
34. Wisse, M., Hobbelen, D., Rotteveel, R., Anderson, S., Zeglin, G.: Ankle springs instead of arc-shaped feet for passive dynamic walkers. In: Proceedings of the 2006 IEEE International Conference on Humanoid Robots, pp. 110–116 (2006)
35. Yamasaki, F., Hosoda, K., Asada, M.: An energy consumption based control for humanoid walking. In: Proceedings of the 2002 IEEE International Conference on Intelligent Robots and Systems, vol. 3, pp. 2473–2477 (2002)
36. Yamasaki, F., Endo, K., Asada, M., Kitano, H.: A control method for humanoid biped walking with limited torque. In: RoboCup 2001: Robot Soccer World Cup V, pp. 60–70. Springer-Verlag, London, UK (2002)
37. Yamasaki, F., Endo, K., Asada, M., Kitano, H.: An energy-efficient walking for a low-cost humanoid robot pino. AI Mag. **23**(1), 60–61 (2002)
38. Yamasaki, F., Endo, K., Kitano, H., Asada, M.: Acquisition of humanoid walking motion using genetic algorithm-considering characteristics of servo modules. In: Proceedings of the 2002 IEEE International Conference on Robotics and Automation, vol. 3, pp. 3123–3128 (2002)
39. Zhao, M., Zhang, J., Dong, H., Liu, Y., Li, L., Su, X.: Humanoid robot gait generation based on limit cycle stability. In: RoboCup 2008: Robot Soccer World Cup XII, pp. 403–413. Springer-Verlag, Berlin, Heidelberg (2009)